An experimental study of exploiting multipath fading for robot communications

Blind Submission. Paper-ID 67

Abstract— A simple approach for mobile robots to exploit multipath fading in order to improve received radio signal strength (RSS), is presented. The strategy is to sample the RSS at discrete points, without deviating too far from the desired position. We first solve the problem of how many samples are needed for given communications performance and how they should be spaced. Second, we propose a circular and a grid trajectory for sampling and give lower bounds on how many samples they will yield. Third, we estimate the parameters of our strategy from measurements. Finally we demonstrate the validity of our analysis through experiments.

I. INTRODUCTION

In many applications for multi-agent robotics, such as surveillance, mapping of unknown environments and searching, the result is of no value unless it can be communicated to a base station or operator. A need arises to ensure that robots perform their tasks in a "communications aware" manner, to avoid losing contact with their team-members or the outside world. There are several approaches to doing this, for example by restricting the movement to preserve connectivity [9], preserving a clear line of sight [1] or deploying relaying agents if the link is getting too weak [16],[15],[11],[2]. Most of the proposed coordination schemes have been developed based on assumptions of very simplified channel models. A popular approach is to use a binary link model where agents can communicate perfectly within a certain radius, but not at all outside it [3]. Slightly more sophisticated approaches assume that the signal strength decays according only to the path loss [12],[10],[6]. In indoor environments, this overlooks the very significant fading effects that have been extensively studied in the field of electromagnetic wave propagation. In this paper, we show that awareness of these effects enables us to make significant improvements in the achieved communications performance for multi-robot systems. There are several other ways of counteracting the multipath fading, such as antenna diversity, adaptive antenna arrays or frequency spreading. But antenna diversity or arrays require a certain physical size of the robot and so may not be feasible for very small platforms. Frequency spreading, on the other hand, is not always very effective, as shown in our measurements and by Puccinelli *et al.* [13].

The contribution of this paper is to formulate the problem of positioning the robot to alleviate the effects of multipath fading, and to validate the proposed approach against real data. The problem is divided into two parts: first we provide an estimate of the number of points that the robot needs to sample to find a position that has a given signal strength. Then we suggest two possible sampling strategies to collect the required

number of independent samples, without deviating too far from the desired path of the robot. It is shown that the approach is robust and works in several kinds of propagation environments, and almost certainly avoids the deep fades where the signal can be attenuated as much as 20 dB. In most cases, the strategy gives a gain of 5 dB or more compared to the local mean signal power. A demonstration in a simple experiment with a single robot is provided.

The proposed coordination mechanism to counteract multipath fading can be interpreted as a software component implementing a connectivity service for an autonomous robot. Frameworks based on software components are essential in the efficient development of large-scale computer systems. Recently its importance has been recognized also for networked embedded systems [2]. A multi-robot application in a disaster relief scenario described in [2] utilizes components for collision avoidance, localization, transmission power control etc. Along those lines, the connectivity service (CS) component would have the task of making small adjustments to the position of the agent to avoid the (very local) reduction of received signal strength because of the multipath fading. For example in a surveillance application, the surveillance component decides on the position of the robot within a certain margin, and the CS component can move the robot within that margin to ensure good communication.

This paper is organized as follows: In Section II, we develop our channel model and explain the phenomenon of multipath fading. We then formally state the problem in Section III and solve it in the case of perfect Rayleigh fading in Section IV. The assumptions for Rayleigh fading are not, in general, true in actual environments, so in Section V we present measurements to estimate the statistical properties of fading in representative environments. Finally we present experimental validation of our approach on a robot platform in Section VI, and end with some conclusions in Section VII.

II. COMMUNICATIONS PRELIMINARIES

In this section we review some results on what determines the received signal strength (RSS) in a radio receiver and how this is affected by the surrounding environment. A good background reference is the book by Stüber [14].

Given a transmission power of P_t, and a distance d to the receiver, the *nominal* signal power P_r in the receiver is

$$P_r(d) = P_t + G_t - PL_0 - 10\ n\ \log_{10} d + G_r\ \text{[dB]}.$$

Here PL_0 is the path loss at 1 m from the antenna and n is the path loss exponent. G_t and G_r are antenna gains in the
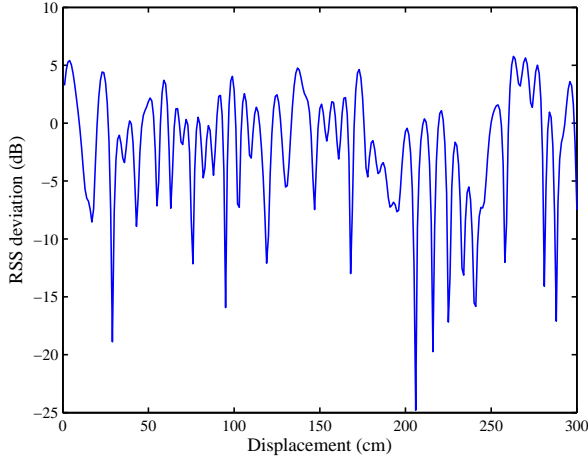
Fig. 1. Simulated Rayleigh fading at 2.4 GHz as the receiver moves along a 3 m line, taking samples of the RSS at every cm.

Fig. 2. Normalized spatial autocorrelation of the RSS in a Rayleigh fading environment.

transmitter and receiver, respectively. The path loss exponent n is 2 for free-space propagation and can reach as high as 4 in some environments. At 2.4 GHz and in an office environment, values around 2.5 have been reported [5].

In an urban or indoor environment, there are however large fluctuations around the nominal level due to shadowing and multipath fading. Shadowing is caused by objects obstructing the signal path and varies over distances the same order as the obstructions. Shadowing is normally modeled as a stochastic process with a log-normal distribution [7].

Multipath fading, on the other hand, is caused by destructive or constructive interference between the signal and its reflections and it varies over very short distances, in the order of a wavelength. Even a stationary receiver will experience multipath fading if the environment is changing, for example due to cars and people moving or doors opening and closing. If all signal components that reach the receiver are of equal strength, the multipath fading is called Rayleigh fading, while if there is a line-of-sight (LoS) component that is significantly stronger, we have Ricean fading. It is worth pointing out that all fading is reciprocal, so it affects the signal path equally in both directions.

Due to the difficulty of predicting the Rayleigh fading, it is usually modeled as a stochastic effect. The probability density function of the power attenuation due to Rayleigh fading is

$$f_P(x) = \frac{1}{P_r} \exp\left(\frac{-x}{P_r}\right). \tag{1}$$

A simulated Rayleigh fading signal power plot is depicted in Figure 1. The spatial autocorrelation of the fading envelope as a function of the distance δ between two samples is

$$R(\delta) = k \, J_0^2(2\pi\delta/\lambda_c), \tag{2}$$

where k is a constant, J_0 is the zero-order Bessel function of the first kind and λ_c is the carrier wavelength. This is illustrated in Figure 2. It shows that two samples taken $0.38\lambda_c$
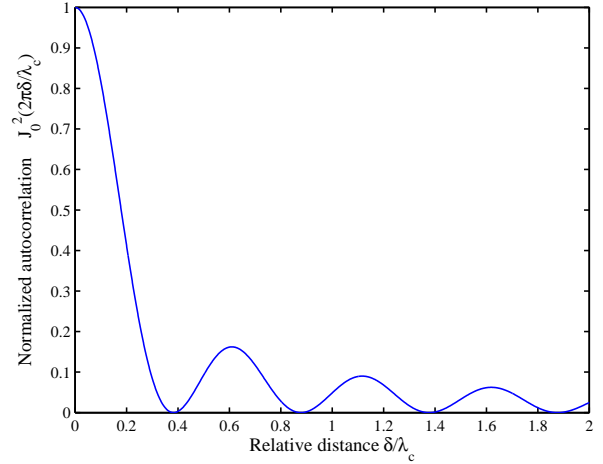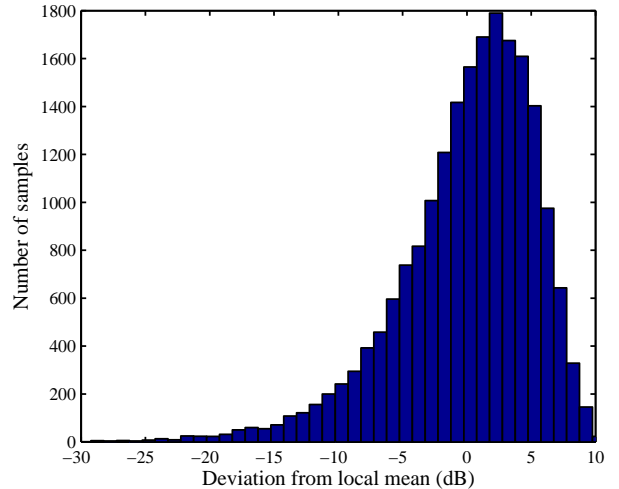

Fig. 3. A histogram based on 2000 simulated measurements, showing the typical Rayleigh distribution.

apart (4.75 cm at 2.4 GHz) should have no covariance, and samples taken at a greater distance should always have small correlations. In practice, samples taken more than about half a wavelength apart are considered to have independent Rayleigh fading. For comparison with measurements in later sections, we also include a histogram of 20000 simulated measurements of Rayleigh fading in Figure 3.

III. PROBLEM FORMULATION

In this section we formulate the problem of coordinating a robot to improve its communication capability by counteracting multipath fading. We consider situations when the application allows the robot to deviate slightly from the desired position, in order to improve the communication. A typical scenario is demonstrated in Figure 4, where robot A monitors
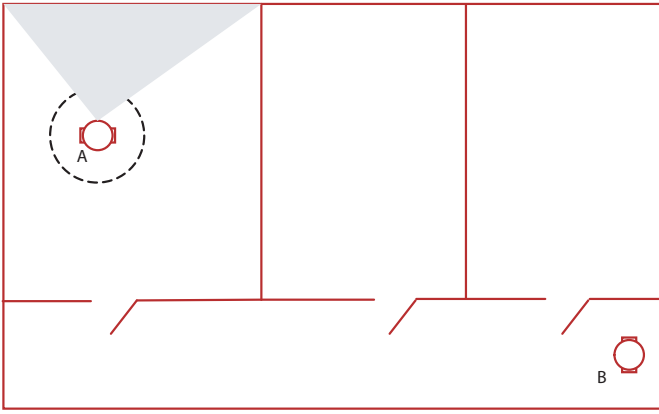
Fig. 4. A scenario where a robot (A) enters a room to monitor part of it, and send the data back to another robot (B). The task can be fulfilled from anywhere inside the dashed circle, so the robot can move inside it to improve the communications with B.

a room and needs to send data to robot B in the corridor outside. The task allows A to deviate within a given region in search of higher signal strength.

Since the RSS is practically impossible to predict and has multiple local maxima, finding the optimal position would require visiting all of the feasible region. We therefore suggest sampling the RSS in a finite number of points, and then going back to the best. This requires high-accuracy navigation, which is not always available. An alternative is to sample a few points to estimate the local average RSS and then continue the sampling, stopping at a point that offers a given improvement over the average. We can then statistically express what improvement of the RSS this will give. Our first problem is thus formulated as:

Problem A: Find the number N of independent samples that we need to get an improvement of G dB over the local average RSS, with probability P.

The trajectory should allow for simple control laws and not deviate outside the feasible region. We have concentrated on what we believe to be the most common robot types today – car-like robots or robots with differential drive. The kinematics of a differential drive robot are

$$\dot{x} = v \cos\theta \qquad (3)$$
$$\dot{y} = v \sin\theta \qquad (4)$$
$$\dot{\theta} = u, \qquad (5)$$

where the robot has position (x, y) and bearing θ, and the control inputs are the angular velocity u and linear velocity v. For car-like robots,

$$u = \frac{v}{L}\tan\alpha, \qquad (6)$$

with L being the distance between rear and front axels, and α the steering angle, limited by $|\alpha| \leq \alpha_{max}$.

Problem B: Find a trajectory that is simple to follow with a car-like or differential drive robot, and offers N sampling points, spaced at least Δ, without deviating more than R from the original position.

As a remark, applications such as transportation or patroling may require the robot to follow a trajectory. In this case the robot may sample the RSS along its trajectory, and stop to communicate when it finds a good position. Problem A is then of interest to give an upper bound on the number of samples (thus also the time or distance) between successful communication attempts.

The general problem has thus been divided into two parts: First finding the number of samples N required to acheive the desired performance and, secondly, finding a suitable trajectory for the robot to visit that many sampling points. In the following, we provide solutions first in the theoretical case of Rayleigh fading, and then based on properties of real enironments.

IV. SOLUTION IN PERFECT RAYLEIGH FADING ENVIRONMENT

In this section we give a solution with provable properties in the case of perfect Rayleigh fading. We first give a proposition on the number of samples required to achieve a certain gain and then suggest two alternative strategies of fitting the required number of independent samples within the region where the robot is allowed to move.

Proposition 4.1 (Number of samples): For a Rayleigh fading environment, the number of independent samples N needed to achieve a power gain of G dB with probability P compared to the local average RSS is given by

$$N = \frac{\ln(1-P)}{\ln(1 - \exp(-10^{G/10}))}.$$

Proof: From Equation 1, we have the pdf of the signal power. With no loss of generality we can assume $P_r = 0$ dB and get the cumulative distribution function (CDF)

$$C(P_n) := \text{Prob}(X < P_n) = 1 - e^{-P_n}$$

i.e., the probability that the power deviation from the local average in a single sample is lower than the threshold P_n. Taking N independent samples, the probability that all of them are lower than P_n is $C(P_n)^N$. We note that at least one sample being greater than P_n is the complementary event to the above, and since $P_n = 10^{G/10}$, the probability of this is

$$\text{Prob}(G) = 1 - \left[1 - \exp(-10^{G/10})\right]^N.$$

Solving for N gives the proposition. □

As described in Section II, samples taken at a distance of $0.38\lambda_c$ can be considered independent. This can be viewed as each sample being surrounded by a disc of radius $0.19\lambda_c$ where no more samples should be taken. So taking N independent samples inside the feasible region with radius R is essentially a two-dimensional sphere-packing problem.

We propose two possible sampling trajectories; driving in a circle and sweeping a hexagonal lattice. They represent different trade-offs between ease of navigation and maximizing the number of samples.
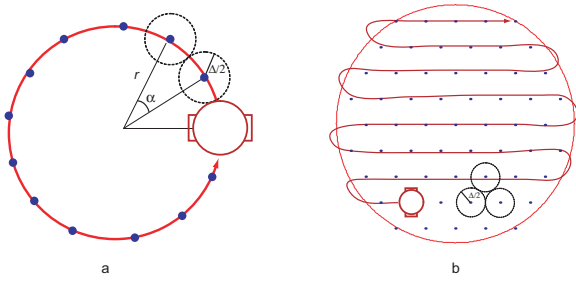
Fig. 5. Two possible sampling trajectories a circle (a) and a hexagonal lattice (b). In both cases, the distance between sampling points is at least Δ.

Proposition 4.2 (Circular sampling trajectory): If N samples are taken on a circle, and the samples are at a distance not less than Δ, the radius of the circle must be

$$r \geq \frac{\Delta}{\sqrt{2}\sqrt{1 - \cos(2\pi/N)}}.$$

Another possible sampling pattern is a hexagonal lattice,

$$\left\{ (x,y) = \Delta(k+a, \ell\sqrt{3}/2) : \begin{cases} a = 0 \text{ if } \ell \text{ even} \\ a = 1/2 \text{ else} \end{cases}, \ k, \ell \in \mathbb{Z} \right\}$$

which was proven by Thue [8] to be optimal for two dimensional sphere-packing. The distance Δ is the vertex distance. This arrangement of sampling points is also suitable for being covered by differential drive or car-like robots. With $\Delta = 0.38\lambda_c$, this would require the robot to drive along parallel lines, spaced $\frac{\sqrt{3}}{2} \, 0.38\lambda_c = 0.33\lambda_c$. In the case of a car-like robot, the line spacing may instead be decided by the minimum turning radius that can be calculated from Equations 3 and 6 as

$$r_{min} = \frac{L}{\tan \alpha_{max}}.$$

A robot equipped with collision sensors also in the back could reverse along every second line, which allows for simple maneuvering. Sensors such as a camera can be pointed in the interesting direction during the whole sampling procedure. If the robot detects an obstacle, it can simply turn earlier and start following the next line back. A hexagonal lattice with sampling trajectory is depicted in Figure 5b. The required size of the sampling region is stated by the following proposition:

Proposition 4.3 (Hexagonal lattice of samples): A hexagonal lattice with vertex distance Δ has at least N vertices within the distance

$$r = \left\lceil \sqrt{\frac{\sqrt{3}(N+1)}{2\pi}} + \frac{1}{\sqrt{3}} \right\rceil \Delta \qquad (7)$$

from the origin.

Proof: Each vertex can be regarded as the center of a hexagon with area $\sqrt{3}\Delta^2/2$. In a circle of radius a, it is possible to place

$$N = \left\lfloor \frac{2\pi a^2}{\sqrt{3}\Delta^2} \right\rfloor$$

such hexagons in a lattice so that at least part of every hexagon fits inside the circle. This can be proven as follows: Assume that any of them is completely outside the circle. Since the remaining hexagons cannot fill the circle, there must be some free space inside, and since hexagons can be tiled with no gaps, this space must be on the perimeter. So the hexagon can be moved there instead.

We also note that no part of a hexagon is more than $\Delta/\sqrt{3}$ from its center. To complete the proof, we note that since all hexagons have some part inside the circle, their centers must then fit inside a concentric circle of radius $a+\Delta/\sqrt{3}$. So solving Equation 7 for a, using that $x+1 \geq \lfloor x \rfloor$ and adding the margin $\Delta/\sqrt{3}$, gives the proposition. $\square$

Other trajectories than the two described here are of course also possible; the fewer samples needed, the greater the flexibility to choose a trajectory.

V. MEASUREMENTS IN REAL ENVIRONMENTS

To apply the proposed strategy in a real environment, we need to estimate the spatial correlation (to determine the sample spacing) and the CDF of the signal strength. We have chosen a basement corridor and a cluttered lab room as representative environments for the measurements.

To automate the measurements, we have mounted a radio based on the CC2420 chip on a robot. It communicates with the same chip on a TMote Sky wireless sensor node, connected to a PC, see Figure 6. The CC2420 operates at 2.4 GHz with a maximal output power of 0 dBm and has a software-accessible received signal strength indicator (RSSI) [4]. It is worth noting that the CC2420 uses direct sequence spread spectrum modulation. This is supposed to alleviate the effects of multipath fading, but as shown below and in [13], the problem of deep fades remains.

The TMote has an antenna integrated on its circuit board, while the robot has a quarter-wave antenna on top. The integrated antenna is by design not omnidirectional, and measurements show that the antenna mounted on the robot also has some directional dependence, due to the influence from the rest of the robot. This makes it important that, when the robot has found the best position and returns there, it also returns to the same orientation.

To estimate the spatial correlation in the different environments, we have driven the robot along straight 200 cm lines, stopping and sampling the RSSI each centimeter. Each sample is formed from averaging the RSSI readings from four radio packets. For each sequence of $N = 200$ samples, we computed the unbiased estimate of the autocorrelation

$$\hat{R}(k) = \frac{1}{N-|k|} \sum_{m=0}^{N-k-1} [z(m) - \bar{z}][z(m+k) - \bar{z}],$$

where $z(n)$ is the signal envelope in sample n and $\bar{z}$ is the mean value.

The CDF of the RSS samples was estimated using the same measurement setup, but driving a distance greater than Δ between samples. We then assumed that the samples could be regarded as independent. After subtracting the average,
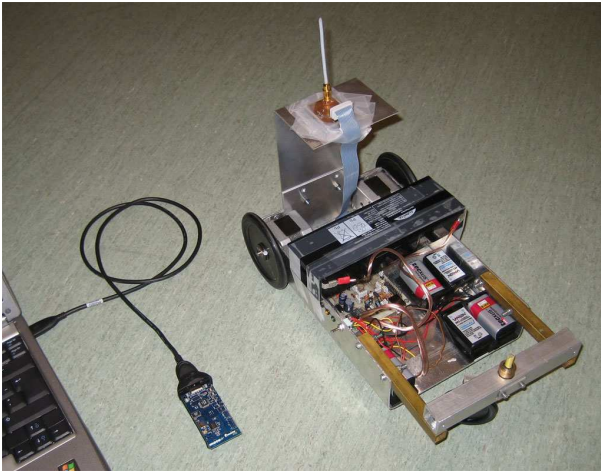
Fig. 6. The measurement system, with the robot and the TMote connected to a PC. The robot has two driving wheels and a third caster wheel, and its antenna is positioned about 25 cm above ground.
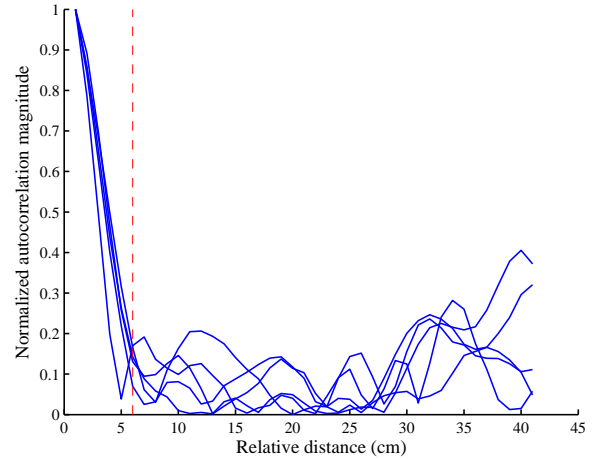

Fig. 8. Autocorrelation estimates for five measurement series in the lab room. The dashed line is the estimated decorrelation distance Δ. The autocorrelation drops rapidly and the spuriouses at 40 cm are probably due to the estimate being noise sensitive at high lags.
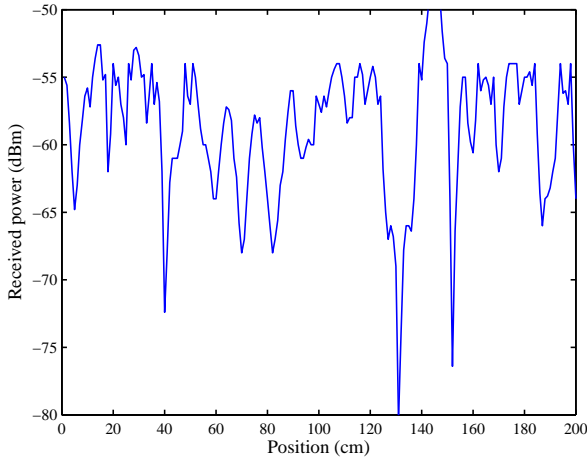

Fig. 7. Measurement results from the lab room, where the RSS varies over 30 dB. Note the deep fade at 130 cm, where the connection was temporarily lost.
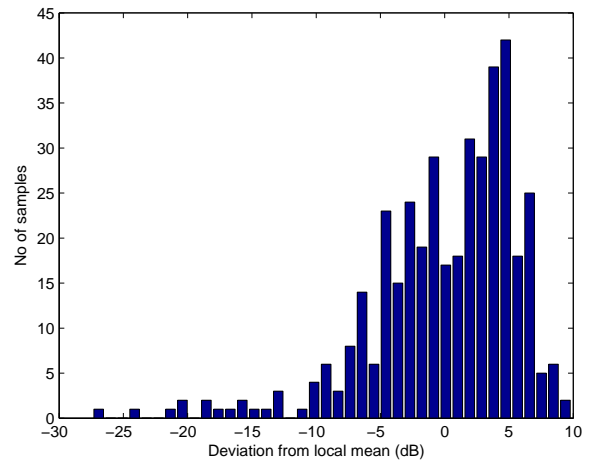

Fig. 9. Histogram of 400 RSS samples, taken in the lab room with sample spacing 10 cm. The distribution resembles the Rayleigh distribution.

we illustrated the result in a histogram. Summing over this histogram gives an estimate of the CDF.

The lab room contains lots of computers, metal cabinets and other effective scatterers, so it is our belief that this environment produces near-Rayleigh fading. This is also confirmed by the measurements. One representative measurement series is depicted in Figure 7, and the estimated autocorrelations for five measurements are superimposed in Figure 8. The autocorrelation decays rapidly, and reaches the noise floor at $\Delta = 6$ cm in all measurements in this environment. (This matches the predicted $\lambda_c/2 = 6.25$ cm.) Finally, the histogram in Figure 9 indicates that the distribution is very similar to the Rayleigh distribution. The samples were taken with a distance of 10 cm to ensure independence.

The corridor has metal grates and cable ducts along its

sides, and large metal cabinets at the entrance. This means that the radio signal may be efficiently reflected from a few large surfaces, so the robot does not receive signals of equal strength from all directions as required for Rayleigh fading. As shown by the measurements, this gives somewhat different spatial properties to the fading. The RSS fluctuates as in the lab room, but also over longer distances, much like shadowing. A representative measurement result is illustrated in Figure 10, and autocorrelation estimates for eight measurements are superimposed in Figure 12. The measurement in Figure 10 corresponds to the slowest decaying autocorrelation estimate. At $\Delta = 15$ cm, all autocorrelation estimates seem to have reached the noise floor for this environment.

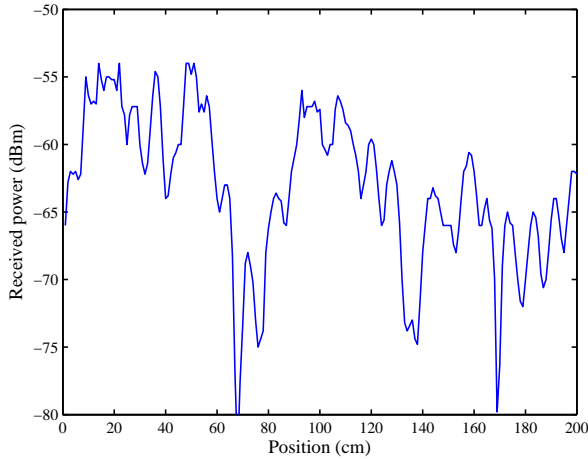To estimate the CDF for the corridor, we took samples 15

Fig. 10. Measurement results from the corridor. The multipath fading is probably superimposed on a shadowing effect.
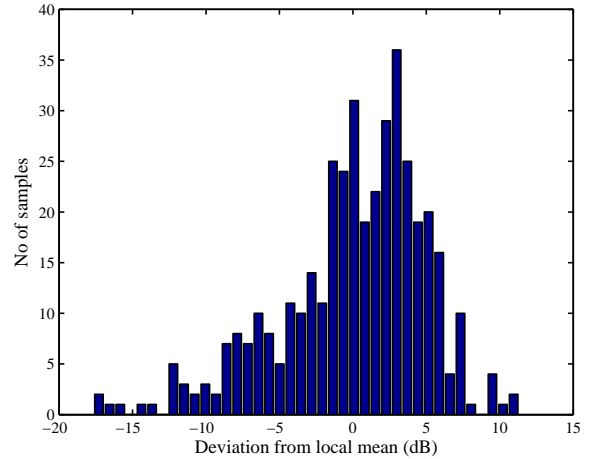

Fig. 12. Histogram of 400 RSS samples, taken in the corridor with sample spacing 15 cm. The distribution resembles the Rayleigh distribution.
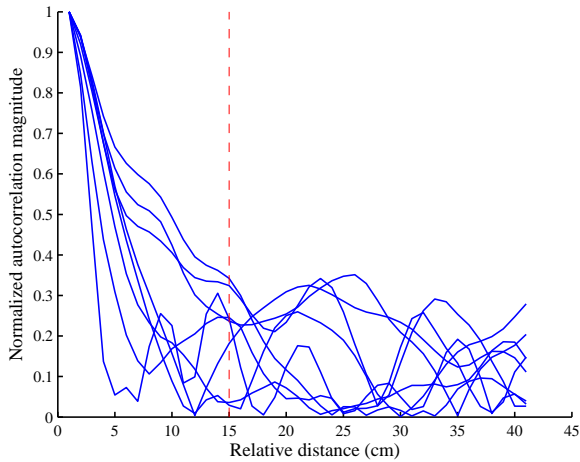

Fig. 11. Autocorrelation estimates for eight measurement series in the corridor. The dashed line is the estimated decorrelation distance Δ. The autocorrelation decays slowly for some series (cf. Figure 8), probably due to shadowing effects.
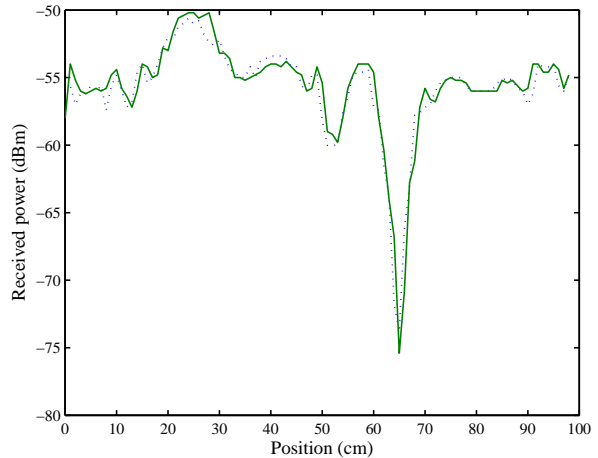

Fig. 13. Two measurement series along the same trajectory. The RSS is clearly a function of the position, and does not vary over time. The RMS deviation between the measurements is 1.15 dB, i.e., within the measurement accuracy.

cm apart and collected them in the histogram in Figure 12. Despite the difference in spatial properties, this distribution also resembles that of Rayleigh fading.

The CC2420 data sheet states an RSSI accuracy of ± 6 dB and linearity within ± 3 dB [4]. Since we are not interested in the absolute signal power, we therefore consider the measurements to have an uncertainty of 3 dB. During our measurements in static environments, the typical standard deviation within 20 packets was less than 1 dB.

Since our motivating application is autonomous exploration or surveillance of indoor environments, we expect those environments to be static. By that we mean that there will be no humans present and little or no movement except for that of the robots themselves. Therefore, the fast fading should not change over time, but only as a function of the position

of the transmitter and receiver. To verify this, we made two measurements, first driving the robot forward 100 cm and then back again along the same line. As illustrated in Figure 13, the RSS as a function of position is very similar between the measurements. The RMS deviation between the measurements is 1.2 dB, i.e., well within the expected uncertainty.

We finally conjectured that the angle between the line of movement and the line connecting the transmitter and receiver did not affect the statistical properties of the RSS. We verified this by doing measurements in several directions during the test in the lab room, and it did not affect the distribution or spatial correlation. Of course this only holds for movements much shorter than the distance to the transmitter, where the
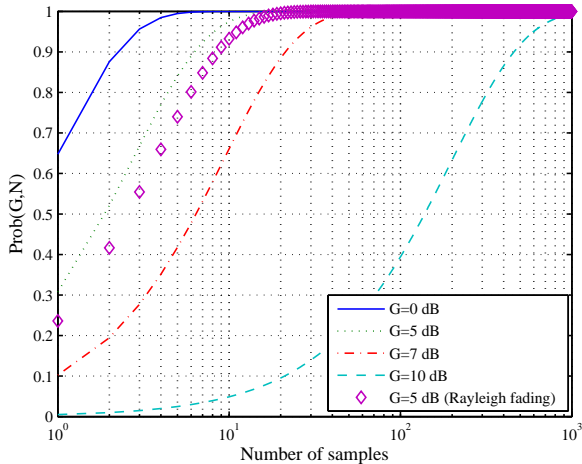
Fig. 14. Results for the lab room: The required number of independent samples of the RSS to achieve a given gain (compared to the local average) with a certain confidence level. We have plotted curves for several gains in the interval 0-10 dB, as well as the corresponding curve for 5 dB in the case of theoretical Rayleigh fading.
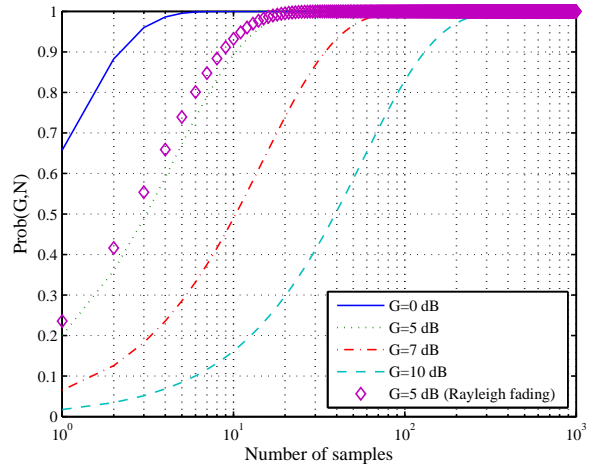

Fig. 15. Results for the corridor: The required number of independent samples of the RSS to achieve a given gain (compared to the local average) with a certain confidence level. We have plotted curves for several gains in the interval 0-10 dB, as well as the corresponding curve for 5 dB in the case of theoretical Rayleigh fading.

change in path loss in negligible.

Using the above measurements, we can compute the estimated CDF $\hat{C}(P_n)$. This yields a result similar to Proposition 4.1, but for this specific environment: The probability of achieving gain G when taking N samples can be estimated as

$$\text{Prob}(G,N) = 1 - \hat{C}(G)^N.$$

Several curves of $\text{Prob}(G,N)$, for some values of G, are plotted for the lab environment as well as the corridor, in Figures 14 and 15, respectively. The corresponding curve for G=5 dB in the case of theoretical Rayleigh fading is added in both graphs as a comparison and it closely matches the corresponding 5 dB-curves for the real environments. These figures summarize the answer to Problem A, showing how many samples are needed to reach a given gain with a specified probability.

In practice this means that if the robot can take approximately 9 samples in the lab room (or 14 in the corridor), it has a 95% chance of finding a position where the signal strength is 5 dB better than the local average. Under the same conditions, the probability of finding a point where the signal strength is at least equal to the local average (and thus avoiding any of the deep fades) is greater than 99.99%. Taking 9 samples in the lab room can be done by going in a circle of radius 8 cm. Conversely, the curves can be used as a guideline for an application designer, choosing the allowed deviation based on what signal gain is needed.

VI. EXPERIMENTAL VERIFICATION

As a simple demonstration of our suggested approach, we have made experiments positioning the robot at random positions and orientations within a 1-by-1 m square in the lab room, as if a task such as patrolling or mapping had made it drive there. We then measured the signal strength between the

robot and its base station (the TMote), in the other end of the room.

First we performed 20 such trials, *series 1*, allowing the robot to deviate slightly from the initial position, sampling the RSS in 9 points, separated by 5 cm. It then moved to the point with the best RSS before the measurement was made. Then we performed 20 more trials, *series 2*, where the robot was not allowed to deviate.

The result of the two experiment series is plotted as two histograms in Figure 16. When just staying at the initial position, seven out of twenty trials yielded signal strengths worse than the local average, in one case by as much as 15 dB. The theoretical analysis predicted a gain of at least 5 dB compared to the local average in 95% of the cases, but in practice this happened in 80% of the trials. It is worth noticing, however, that all trials avoided negative gains as predicted.

To illustrate the benefit of gaining 5 dB, we quote an expression for the packet reception rate (PRR) as function of the signal-to-noise ratio (SNR), derived by Zuniga *et al.* [17]. They use MICA2 motes (which work at lower frequencies but have similar performance as the TMotes) with a data rate of 19.2 kbps and a PRR of

$$p(SNR) = \left(1 - 1/2e^{-\frac{SNR}{1.28}}\right)^{8f},$$

where f is the frame size, i.e., the number of bytes in each packet. With a frame size of $f = 50$, a MICA2 mote on the limit of losing contact, with SNR=5 dB, would receive 1.8% of the packets and thus have an effective bandwidth of 340 bits/s. Sending a 10 kbyte camera image would then take 3 min 55 s. Gaining 5 dB would raise the bandwidth to 17.7 kbits/s, reducing the sending time to 4.5 seconds.
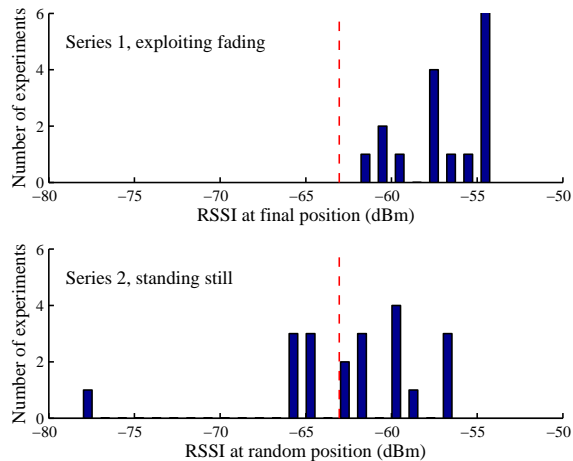
Fig. 16. Experiment results, measuring the RSS at the final position of the robot. The upper histogram shows the result when using the proposed approach, and the lower histogram shows what happened when the robot did not move from its (random) original position. The dashed line shows the local average RSS.

VII. CONCLUSION AND FUTURE WORK

We have formulated the problem of positioning an autonomous robot to avoid the negative effect of multipath fading in radio communication. The problem is divided into two parts: first we provide an estimate of the number of points that it needs to sample to find a position that has a given signal strength. Then we suggest two possible sampling strategies to collect the required number of independent samples, without deviating too far from the original position.

This is a robust approach that works in several kinds of propagation environments and almost certainly avoids the deep fades where the signal can be attenuated as much as 20 dB. In most cases it also gives a gain of 5 dB or more compared to the local mean signal power. This can be interpreted as using the unstructured environment as a directional antenna. The performance of this strategy was demonstrated in a simple experiment.

As mentioned in the introduction, the problem of multipath fading can also be countered in other ways, for example by antenna diversity as used in WLAN base stations. Our approach can be seen as a sort of antenna diversity over time, in case the robot is too small to host two antennas separated by at least half a wavelength. This also motivates moving groups of robots in hexagonal lattice formations with distance Δ between agents. Such a lattice represents the tightest possible formation offering antenna diversity gain for the group as a whole: ensuring that at least some of the robots have good signal strength.

In the future we would like to find criteria for how the variance of the RSS over time can be used to detect that the environment is no longer static. Then the robot could adapt its strategy to increase the search space, exploit shadow fading instead or simply stop making adjustments to its position. It

would also be a warning to the user that the performance of the algorithm cannot be guaranteed in those cases. Finally, we would like to measure the fading properties of other environments to further validate our approach.

REFERENCES

[1] R. Arkin and T. Balch. Line-of-sight constrained exploration for reactive multiagent robotic teams. 7th International Workshop on Advanced Motion Control, July 2002. Maribor, Slovenia.

[2] K.-E. Årzén, A. Bicchi, G. Dini, S. Hailes, K.H. Johansson, J. Lygeros, and A. Tzes. A component-based approach to the design of networked control systems. European Journal of Control, 2007. To appear.

[3] Z. Butler and D. Rus. Event-based motion control for mobile sensor networks. IEEE Pervasive Computing, 2(4), 2003.

[4] Chipcon AS. CC2420 Datasheet 1.4. www.chipcon.com, 2006.

[5] F. Darbari, I. McGregor, G. Whyte, R. W. Stewart, and I. Thayne. Channel estimation for short range wireless sensor network. In Proceedings of the 2nd IEE/Eurasip Conference on DSP Enabled Radio, 2005. UK, September.

[6] A. Drenner, I. Burtz, B. Kratochvil, B. J. Nelson, N. Papanikolopoulos, and K. B. Yesin. Communication and mobility enhancements to the scout robot. In Proceeding of the IEEE/RSJ International Conference on Intelligent Robots and System, 2002. Lausanne, Switzerland, September-October.

[7] M. Gudmundson. Analysis of handover algorithms [microcellular radio]. In Proceedings of the IEEE Vehicular Technology Conference, 1991. May 19-22.

[8] T. C. Hales. An overview of the Kepler conjecture. http://www.math.pitt.edu/ thales/kepler98/sphere0.ps, 1998.

[9] M. A. Hsieh, A. Cowley, V. Kumar, and C. J. Taylor. Towards the deployment of a mobile robot network with end-to-end performance guarantees. In Proceedings of the IEEE International Conference on Robotics and Automation, 2006. Orlando, Florida, May 2006.

[10] M. F. Mysorewala, D.O. Popa, V. Giordano, and F.L. Lewis. Deployment algorithms and in-door experimental vehicles for studying mobile wireless sensor networks. In Proceedings of the7th ACIS International Conference on Software Engineering, Artificial Intelligence, Networking, and Parallel/Distributed Computing, 2006. Las Vegas, Nevada, June.

[11] H. G. Nguyen, N. Farrington, and N. Pezeshkian. Maintaining Communication Link for Tactical Ground Robots. In AUVSI Unmanned Systems North America, 2004.

[12] D. O. Popa and C. Helm. Robotic deployment of sensor networks using potential fields. In Proceedings of the IEEE International Conference on Robotics & Automation, 2004. New Orleans, LA, April.

[13] D. Puccinelli and M. Haenggi. Multipath fading in wireless sensor networks: Measurements and interpretation. In Proceedings of the International Wireless Communications and Mobile Computing Conference, 2006. July 3-6, Vancouver, Canada.

[14] Gordon L. Stüber. Principles of mobile communication. Kluwer academic publishers, 1996.

[15] J.D. Sweeney, R.A. Grupen, and P. Shenoy. Active QoS flow maintenance in controlled mobile networks. In Proceedings of the Fourth International Symposium on Robotics and Automation, 2004. Queretaro, Mexico, August 2004.

[16] A. Wagner and R. Arkin. Multi-robot communication-sensitive reconnaissance. In Proceedings of the IEEE International Conference on Robotics and Automation, 2004. New Orleans, LA, April 2004.

[17] M. Zuniga and B. Krishnamachari. Analyzing the transitional region in low power wireless links. In Proceedings of the First IEEE International Conference on Sensor and Ad hoc Communications and Networks, 2004. Santa Clara, CA, October 2004.